



Theory of the impedance of charge transfer via surface states in dye-sensitized solar cells

Juan Bisquert^{*}

Photovoltaic and Optoelectronic Devices Group, Departament de Física, Universitat Jaume I, 12071 Castelló, Spain

ARTICLE INFO

Article history:

Received 8 September 2009

Received in revised form 24 December 2009

Accepted 8 January 2010

Available online 18 January 2010

Keywords:

Dye solar cell

Impedance Spectroscopy

Surface states

Nanostructures

ABSTRACT

The dynamics of trapping coupled with charge transfer is analysed in the frequency domain for a model of the dye-sensitized solar cell. We solve the steady state occupations of the surface state and the resulting recombination currents, based on the assumption of detailed balance. We determine all the parameters that control the frequency response in Impedance Spectroscopy as a function of the steady state, and the characteristic shape of the impedance spectra. At large charge transfer rate the low frequency capacitance of the surface states is considerably reduced with respect to the thermodynamically defined equilibrium capacitance. We also show that the usual kinetics of recombination does not give a negative capacitance contribution.

© 2010 Elsevier B.V. All rights reserved.

1. Introduction

Considerable research effort has been devoted to the dye-sensitized solar cell (DSC) based on mesoporous titania, as a feasible low cost photovoltaic device. DSC devices with ruthenium sensitizers and liquid electrolytes have achieved demonstrated efficiencies over 11% at 1 full sun, and remarkable stability has been obtained using ionic liquids. In a DSC, electrons injected into mesoscopic TiO₂ recombine with the holes in the redox carrier or organic solid conductor by interfacial charge transfer. It is believed that a better understanding of the back reaction of photoinjected electrons may contribute to greatly improve device performance, and especially photovoltages, by a rational design of materials and nanostructures [1].

It was recognized that surface states play a dominant role in electrochemical reactions at extrinsic crystalline semiconductor electrodes [2–5]. In a DSC, low doped anatase-TiO₂ nanoparticles ca. 20 nm diameter are frequently used to form the porous semiconductor electron transport phase. Such particles present both a large surface exposed to the hole transport material, and prominent energy disorder in the electronic states that becomes apparent in different kinds of dynamic measurements [1,6]. It has therefore been established that most of the electrons reside in localized states in the bandgap. Since a distance for electron tunneling should be of the order of 1 nm, it is important to consider in detail the dynamics of charge transfer from bandgap localized

states situated close to the surface of the nanoparticle, within tunneling reach (hereafter termed *surface states*), to the electron acceptor.

Small amplitude perturbation dynamic techniques have become a major tool for DSC characterization [7,8]. In the literature of photoelectrochemistry there are detailed treatment of the dynamic effects of surface states [4,9–15]. We have presented calculations of the effect of surface states in DSC in steady state [16–18], and we have also characterized quite generally the dynamics of traps in terms of Impedance Spectroscopy (IS) [19,20]. However, the combination of trapping and charge transfer in surface states introduces additional features in the dynamics [2–5]. IS of charge transfer via surface states has been mentioned sometimes in the DSC field but the traps dynamics was not explicitly described [21,22].

Recently some IS experimental evidence has been presented for charge transfer involving a distribution of surface states in DSC with volatile electrolytes [8,23], and via a localized surface state in the case of aqueous electrolyte [24] and ionic liquids [25]. Another important feature of IS measurements in DSC is the frequent observation of a negative capacitance at low frequencies [26]. This is obtained in different types of solar cells, for example in DSC with OMETAD solid hole conductor [27] and in mesoscopic TiO₂ quantum dot-sensitized solar cells [24]. This feature greatly complicates the analysis and interpretation of steady state performance of the investigated DSCs. A recent experimental study shows the progressive suppression of the negative capacitance by conformal covering of the TiO₂ with an insulator phase, via atomic layer deposition [27]. It is therefore likely that the negative capacitance is strongly

^{*} Tel.: +34 630754638.

E-mail address: bisquert@fca.uji.es

connected to the recombination via surface states, but a definite model to support this has not been devised so far.

Let us summarize briefly the basic features of the known IS models for DSC concerning recombination and traps (neglecting diffusion). The potential applied in the mesoporous TiO_2 produces a charging of the chemical capacitance of the transport states [28]. Charge transfer from the transport state produces a recombination resistance in parallel with the chemical capacitance [29]. A trap is a localized state in the bandgap that communicates with the transport state. The trap has a separate chemical capacitance [30], that is connected in parallel to the chemical capacitance of the conduction band states. Trapping and detrapping also has a resistive component, and the equivalent circuit for a trap consists on a series of resistance and the chemical capacitance of the trap [9,20].

Additional features, due to the charge transfer from the trap are analysed in this paper. We discuss the kinetic response as a function of the occupation of the states in the model shown in Fig. 1 of a mesoporous semiconductor that contains a transport state that can be controlled by the potential applied in the substrate, and a localized surface state. To simplify the treatment, and focus on the required features, diffusion in the transport state is assumed infinitely fast, and band unpinning (a property often considered in photoelectrochemistry [12,15]) is neglected as well. These features are briefly commented in the final section of the paper. Trapping–detrapping kinetics is formulated in terms of conventional detailed balance assumption [31]. Both the free and localized state

produce charge transfer to the hole transport phase, and this constitutes a basic description of recombination in a DSC [23]. We describe fully both the steady state features, by determining the statistics of occupation, and the equivalent circuits that allow the interpretation of the frequency measurements. Therefore we can predict how the equivalent circuit parameters vary with the external bias voltage.

2. Model

2.1. The general kinetic equations

Fig. 1 shows a piece of nanostructured semiconductor in contact with a conducting substrate at the left side. A transport level (conduction band edge at the level E_c) allows the displacement of electrons through the mesostructure. Charge transfer to acceptor species in solution may occur in two different pathways: by direct transfer from extended states in the conduction band, and via surface states. We first assume that surface states are concentrated at a single energy level, E_t , and a distribution of surface states that usually occurs in DSC, is treated later on.

The surface states are connected by trapping–detrapping kinetics to the transport level, that communicates with the outer contact. In the scheme, we indicate that the potential V governs the Fermi level E_F as

$$qV = E_F - E_{redox} \quad (1)$$

where q is the elementary charge. The Fermi level in the unbiased system, E_{F0} , is equilibrated with E_{redox} , the redox potential of the holes in solution. The extended states have an effective density N_c and number density of carriers n_c , given by

$$n_c = N_c e^{(E_F - E_c)/k_B T} = n_0 e^{qV/k_B T} \quad (2)$$

where k_B is Boltzmann's constant, T is the temperature and n_0 is an equilibrium density at zero bias.

The kinetics of electrons in the surface state is governed by the equation that describes the variation of the occupancy function of the state, f_{ss} , due to trapping and release from the transport state, and transfer of electrons to the hole acceptor:

$$\frac{\partial f_{ss}}{\partial t} = \beta_c n_c [1 - f_{ss}] - \varepsilon_r f_{ss} - k_{ss} (f_{ss} - f_{ss0}) \quad (3)$$

Here β_c is the time constant for electron capture, ε_r the constant for release, and k_{ss} the rate constant for charge transfer. By detailed balance condition, in equilibrium without applied bias each exchange process must be separately balanced. For the charge transfer process we have obviously $f_{ss} = f_{ss0} = f_{ss}(E_{F0})$, and for the trapping process we obtain from Eq. (3)

$$f_{ss0} = \frac{1}{1 + \varepsilon_r / (\beta_c n_0)} \quad (4)$$

In equilibrium we also have $f_{ss0} = F(E_t, E_{F0})$, in terms of the Fermi–Dirac function

$$F(E, E_F) = \frac{1}{1 + e^{(E - E_F)/k_B T}} \quad (5)$$

Therefore the following constraint holds

$$\varepsilon_r(E_t) = \beta_c N_c e^{(E_t - E_c)/k_B T} = \beta_c n_c e^{(E_t - E_F)/k_B T} \quad (6)$$

We consider the kinetics of electrons in the transport level in the mesoporous semiconductor of thickness L shown in Fig. 1a. At position x , J_n is the flux of carriers in the positive x direction by diffusion, that relates to the gradient of concentration by Fick's law

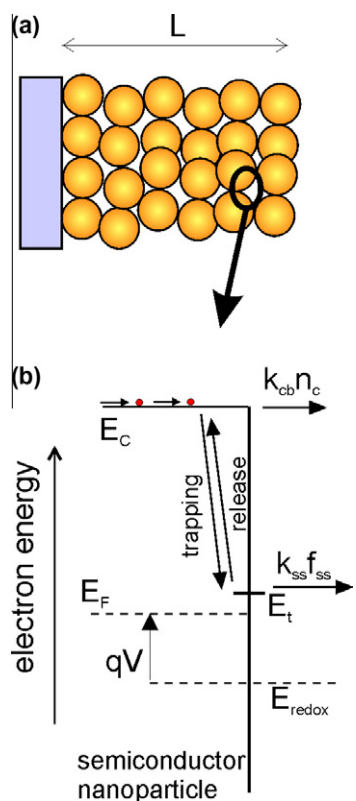


Fig. 1. (a) Mesoporous semiconductor film deposited over a conducting substrate, the matrix of the active layer in a DSC. (b) Schematic representation of the steps involved in the recombination between the electrons in TiO_2 nanoparticles and the oxidized species (holes) in the electrolyte. E_F is the Fermi level of electrons under illumination and E_c is the transport level (conduction band) energy, E_{redox} is the redox potential of the acceptor species in solution, and E_t is the energy level of a surface state in the bandgap. The following steps are indicated: electron transport; electron transfer through conduction band; capture and release by a surface state; electron transfer from the surface state. The rate of interfacial charge transfer from transport states is $k_{cb} n_c$ and the rate of charge transfer from the surface state is $k_{ss} f_{ss}$.

$$J_n = -D_0 \frac{\partial n}{\partial x} \quad (7)$$

Here D_0 is the diffusion coefficient electrons. The variation of electron density at point x is determined by the change of the flux, and by trapping, release and charge transfer terms:

$$\frac{\partial n_c}{\partial t} = -\frac{\partial J_n}{\partial x} - \beta_c n_c N_{ss} [1 - f_{ss}] + \varepsilon_r N_{ss} f_{ss} - k_{cb} n_c \quad (8)$$

2.2. The global dynamic equation

Eqs. (3) and (8) form a general model for transport, trapping and charge transfer. Solving the model requires due consideration of generation terms (this has been omitted in Eq. (8), since it provides a trivial modification of the IS results) and the boundary conditions. In this paper we are interested in the local behaviour of trapping and charge transfer. Therefore we adopt some simplifying assumptions to obtain the steady state and impedance response of the mesoporous film, neglecting the transport phenomena, which can be added if desired in a more complete model (the impedance of diffusion and diffusion-trapping has been amply described [19,20,29]). We assume that D_0 is very large implying that the gradient of concentration required to maintain the flux is very small. With these assumptions n_c and f_{ss} become independent of position. We now integrate between $0 \leq x \leq L$ and obtain

$$\frac{\partial n_c}{\partial t} = -\frac{1}{L} [J_n(L) - J_n(0)] - \beta_c n_c N_{ss} [1 - f_{ss}] + \varepsilon_r N_{ss} f_{ss} - k_{cb} n_c \quad (9)$$

For the boundary conditions we assume that the mesoporous semiconductor in Fig. 1 is supplemented with ideal selective contacts to form a DSC [32]. The left contact is reversible to electrons as already stated in Eq. (2), and electrical current density at this contact is given by

$$j = -qJ_n(0) \quad (10)$$

The electron flux is blocked at the right boundary, Fig. 1a, therefore

$$J_n(L) = 0 \quad (11)$$

Using Eqs. (3), (10) and (11), we obtain from Eq. (9) the dynamic equation that relates the variation of local, homogeneous concentrations (in transport and trap states) to the current injected or extracted from the mesoporous film.

$$\frac{j}{qL} = -\frac{\partial}{\partial t} (n_c + N_{ss} f_{ss}) - k_{ss} N_{ss} f_{ss} - k_{cb} n_c \quad (12)$$

Eq. (12) describes the current injected or extracted in the film in terms of (a) charging of electronic states (first term) and (b) electron flow out of the film by charge transfer (second and third terms). Eq. (12) in combination with the trap dynamics in (3) form the basis for the subsequent model calculations in this paper.

We will distinguish two types of experimental conditions. One is the steady state condition at applied bias, and the quantities in such conditions are denoted \bar{y} , if required. The second type is a small harmonic perturbation of angular frequency ω and frequency $f = \omega/2\pi$. The amplitudes of small perturbation are denoted by \hat{y} .

2.3. Steady state quantities

At steady state with an applied bias we will assume for simplicity that $\bar{f}_{ss} \gg \bar{f}_{ss0}$. Eq. (3) reduces to

$$\beta_c \bar{n}_c [1 - \bar{f}_{ss}] - \varepsilon_r \bar{f}_{ss} - k_{ss} \bar{f}_{ss} = 0 \quad (13)$$

or

$$\beta_c \bar{n}_c = (\beta_c \bar{n}_c + \varepsilon_r + k_{ss}) \bar{f}_{ss} \quad (14)$$

The occupancy of the surface state is

$$\bar{f}_{ss} = \frac{1}{1 + \frac{\varepsilon_r + k_{ss}}{\beta_c \bar{n}_c}} = \frac{1}{1 + (1 + k_{ss}/\varepsilon_r) e^{-(E_F - E_t)/k_B T}} \quad (15)$$

In contrast with (4), Eq. (15) no longer has the form of the Fermi–Dirac function relative to E_t , due to the fact that electrons are continuously transferred to the hole transport medium. In fact when $E_F < E_t$ and $k_{ss} > \varepsilon_r$ the standard, Boltzmann occupation is reduced as follows:

$$\bar{f}_{ss} \approx \frac{\varepsilon_r}{k_{ss}} e^{(E_F - E_t)/k_B T} \quad (16)$$

The Fermi level of the surface states is lower than that of transport states, as discussed in Ref. [16].

At steady state, electronic states attain their equilibria with respect to the imposed voltage, Eqs. (2) and (15). Therefore all the current is recombination current. From Eq. (12), and omitting the overbars, we have

$$j_{rec} = -qL[k_{ss} N_{ss} f_{ss} + k_{cb} n_c] \quad (17)$$

Let us calculate the following useful derivatives

$$\frac{dn_c}{dV} = -\frac{q}{k_B T} n_c \quad (18)$$

$$\frac{df_{ss}}{dV} = -\frac{q}{k_B T} f_{ss} (1 - f_{ss}) \quad (19)$$

Now we can obtain from (17) the recombination resistance,

$$r_{rec}^{-1} = \frac{\partial j}{\partial V} = [r_{rec}^{(cb)}]^{-1} + [r_{rec}^{(ss)}]^{-1} \quad (20)$$

where we have stated separately the recombination resistances for conduction band and surface states

$$[r_{rec}^{(cb)}]^{-1} = \frac{q^2 L}{k_B T} k_{cb} n_c \quad (21)$$

$$[r_{rec}^{(ss)}]^{-1} = \frac{q^2 L}{k_B T} k_{ss} N_{ss} f_{ss} (1 - f_{ss}) \quad (22)$$

It is also important to determine the chemical capacitance for transport states and trap states. Using again Eqs. (18) and (19), we obtain [6,28] the following *equilibrium* chemical capacitances for the conduction band and surface states:

$$C_{\mu}^{(cb)} = qL \frac{d\bar{n}_c}{dV} = \frac{q^2 L}{k_B T} n_c \quad (23)$$

$$C_{\mu eq}^{(ss)} = qLN_{ss} \frac{d\bar{f}_{ss}}{dV} = \frac{q^2 L}{k_B T} N_{ss} f_{ss} (1 - f_{ss}) \quad (24)$$

We note that Eqs. (23) and (24) are defined quite generally based on thermodynamic arguments (see Eq. (1.4) in [33]). The capacitance $C_{\mu eq}^{(ss)}$ is indeed measured at low frequency [30] provided that there is no charge transfer from the surface state. The measured capacitance at low frequency is discussed generally below.

Combining Eqs. (21) and (23) we get the relationship [23]

$$r_{rec}^{(cb)} C_{\mu}^{(cb)} = k_{cb}^{-1} \quad (25)$$

and similarly

$$r_{rec}^{(ss)} C_{\mu eq}^{(ss)} = k_{ss}^{-1} \quad (26)$$

We note here a third important relationship

$$r_{td}^{(ss)} C_{\mu eq}^{(ss)} = \omega_t^{-1} \quad (27)$$

where $r_{td}^{(ss)}$ is the resistance for trapping–detrapping, and ω_t is the frequency of the trap. Both magnitudes are defined later on.

2.4. Calculation of the impedance

We first take the equation for trap kinetics, (3), and express it for a small perturbation in the frequency domain ($\partial/\partial t \rightarrow i\omega$). Rearranging the terms in \hat{f}_{ss} and \hat{n}_c , we obtain

$$[i\omega + \beta_c \bar{n}_c + \varepsilon_r + k_{ss}] \hat{f}_{ss} = [1 - \bar{f}_{ss}] \beta_c \hat{n}_c \quad (28)$$

Using the steady state Eq. (14), Eq. (28) takes the form [20]

$$\hat{f}_{ss} = \frac{1}{\bar{n}_c} \frac{\bar{f}_{ss}(1 - \bar{f}_{ss})}{1 + i\omega/\omega_t} \hat{n}_c \quad (29)$$

where the characteristic frequency of the trap is defined as

$$\omega_t = \frac{\varepsilon_r + k_{ss}}{1 - \bar{f}_{ss}} = \frac{\beta_c n_c}{\bar{f}_{ss}} \quad (30)$$

and it has the value

$$\omega_t = (\beta_c n_c + \varepsilon + k_{ss}) \quad (31)$$

Note also the following relationship between the small perturbation of free electron density, and voltage:

$$\hat{n}_c = \frac{d\bar{n}_c}{dV} \hat{V} = -\frac{C_{\mu}^{(cb)}}{qL} \hat{V} \quad (32)$$

Therefore from (29) we can write

$$\hat{f}_{ss} = -\frac{1}{LqN_{ss}} \frac{C_{\mu eq}^{(ss)}}{1 + i\omega/\omega_t} \hat{V} \quad (33)$$

Now we take the general dynamic Eq. (12). For a small perturbation this gives

$$\frac{\hat{j}}{qL} = -[i\omega + k_{cb}] \hat{n}_c - N_{ss} [i\omega + k_{ss}] \hat{f}_{ss} \quad (34)$$

We substitute Eqs. (32) and (33) to leave the voltage as the only variable. Then the impedance is calculated from Eq. (34) as

$$Z_{tot} = \frac{\hat{V}}{\hat{j}} = \frac{1}{C_{\mu}^{(cb)} [k_{cb} + i\omega] + C_{\mu eq}^{(ss)} \frac{k_{ss} + i\omega}{1 + i\omega/\omega_t}} \quad (35)$$

Let us write this last result as

$$Z_{tot} = \frac{1}{i\omega C_{\mu}^{(cb)} + [r_{rec}^{(cb)}]^{-1} + Z_{ss}^{-1}} \quad (36)$$

where

$$Z_{ss} = \frac{1}{C_{\mu eq}^{(ss)} \frac{1 + i\omega/\omega_t}{k_{ss} + i\omega}} \quad (37)$$

The following alternative derivation of the same result is useful for generalizations. We express Eq. (34) as

$$\hat{j} = C_{\mu}^{(cb)} \left[i\omega + k_{cb} + \beta_c N_{ss} (1 - \bar{f}_{ss}) - N_{ss} (\beta_c \bar{n}_c + \varepsilon_r) \frac{\hat{f}_{ss}}{\bar{n}_c} \right] \hat{V} \quad (38)$$

Therefore

$$Y_{tot} = \frac{\hat{j}}{\hat{V}} = i\omega C_{\mu}^{(cb)} + [r_{rec}^{(cb)}]^{-1} + Y_{ss} \quad (39)$$

and

$$Y_{ss} = N_{ss} C_{\mu}^{(cb)} \left[\beta_c (1 - \bar{f}_{ss}) - (\beta_c \bar{n}_c + \varepsilon_r) \frac{\hat{f}_{ss}}{\bar{n}_c} \right] \quad (40)$$

If we apply Eqs. (14) and (29), Eq. (40) becomes identical with (37). Eq. (40) shows that the trap subcircuit is totally determined by the kinetic equation of the trap (which gives \hat{f}_{ss}/\bar{n}_c), independently of the specific mechanism whereby the external potential modulates the free carrier concentration (this may involve diffusion or other processes, in more complex device models). Therefore the results obtained here for Z_{ss} can be applied in more general IS device models.

2.5. Equivalent circuit representations and low frequency limit

Eq. (35) implies that the impedance of the model of Eq. (12) consists of three parallel contributions, as indicated in Fig. 2a.

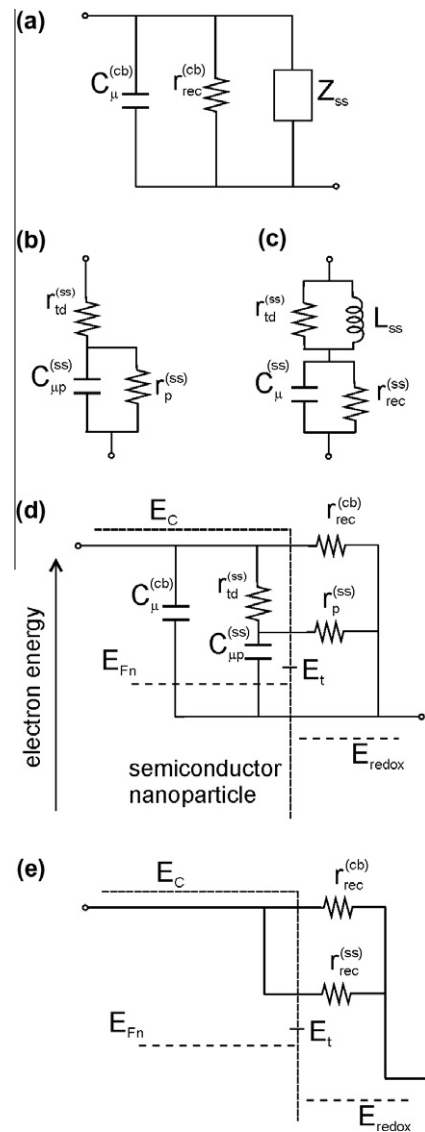


Fig. 2. (a) Equivalent circuit for ac impedance conditions in the model of Fig. 1b with electron transfer both from conduction band (E_c) and a surface state in the bandgap at energy E_t . (b) and (c) are different representations of the traps impedance Z_{ss} . (d) Scheme showing the physical interpretation the equivalent circuit in (b). $C_{\mu}^{(cb)}$ is the chemical capacitance of free carriers, $r_{rec}^{(cb)}$ is the recombination resistance of free carriers, $r_{td}^{(ss)}$ is the resistance for trapping and detrapping, $C_{\mu p}^{(ss)}$ is a parallel capacitance of the surface state, $r_p^{(ss)}$ is a parallel resistance from the surface state. (e) The equivalent circuit for stationary (dc) conditions. $r_{rec}^{(ss)}$ is the recombination resistance from the surface state.

The first is the capacitance of the conduction band, that describes potentiostatic charging of the transport states, as illustrated in Fig. 2d. The second element is the resistance for charge transfer from the conduction band. These two elements are standard for all solar cells [23,28]. The third element is the impedance of the traps, Eq. (37), that can be written as

$$Z_{ss} = r_{td}^{(ss)} + \frac{1}{\left[r_p^{(ss)}\right]^{-1} + i\omega C_{\mu p}^{(ss)}} \quad (41)$$

Here, the resistance for trapping–detrapping $r_{td}^{(ss)}$ is defined by Eqs. (27) and (30),

$$\left[r_{td}^{(ss)}\right]^{-1} = \frac{q^2 L}{k_B T} N_{ss} (\varepsilon_r + k_{ss}) \bar{f}_{ss} \quad (42)$$

and

$$C_{\mu p}^{(ss)} = B^{-1} C_{\mu eq}^{(ss)} \quad (43)$$

$$r_p^{(ss)} = B r_{rec}^{(ss)} \quad (44)$$

$$B = \left(1 - \frac{k_{ss}}{\omega_t}\right) \quad (45)$$

Eq. (41) shows the structure of the impedance of the surface states. It is given by the resistance of trapping–detrapping, in series with two parallel elements, a capacitance and a resistance, defined in Eqs. (43) and (44). This is indicated in Fig. 2b and d.

The representation of Z_{ss} in Fig. 2b is not unique, and the equivalent subcircuit for the trap impedance can be expressed in several equivalent ways. For example we can write Eq. (37) also as

$$Z_{ss} = \frac{1}{\left[r_{rec}^{(ss)}\right]^{-1} + i\omega C_{\mu eq}^{(ss)}} + \frac{1}{\left[r_{td}^{(ss)}\right]^{-1} + \frac{k_{ss}}{r_{td}^{(ss)} i\omega}} \quad (46)$$

This is a series of two parallel circuits, Fig. 2c, and the upper one consists on a resistance and an inductor with the value

$$L_{ss} = \frac{r_{td}^{(ss)}}{k_{ss}} = \frac{k_B T}{q^2 L N_{ss} \bar{f}_{ss} k_{ss} (\varepsilon_r + k_{ss})} \quad (47)$$

The presence of an inductor in the equivalent circuit, noted by Cardon in 1972 (who provides yet another equivalent circuit [10]), introduces the possibility that the impedance takes values in the fourth quadrant of the complex plot, i.e. $-Z'' = -\text{Im}(Z) < 0$. It also appears at first sight that if $k_{ss} > \omega_t$ both $C_{\mu p}^{(ss)}$ and $r_p^{(ss)}$ in Eqs. (43) and (44) can be *negative*. However, using the form of the trap frequency, Eq. (30), it is found that the factor B is always positive

$$B = \frac{1}{1 + \frac{k_{ss}}{\varepsilon_r + \beta_c n_c}} = \frac{\varepsilon_r + \bar{f}_{ss} k_{ss}}{\varepsilon_r + k_{ss}} \quad (48)$$

and takes, approximately, the following values:

$$B \approx \frac{\varepsilon_r}{k_{ss}} \quad \text{if } E_F < E_t \quad (49)$$

$$B \approx 1 \quad \text{if } E_F > E_t \quad (50)$$

Since the impedance can be expressed in terms of (positive) resistors and capacitors, it will be restricted to the first quadrant, $[Z' = \text{Re}(Z) > 0, -Z'' > 0]$. To further investigate this point, let us calculate the low frequency value of the impedance. At low frequency

$$Z_{ss}(\omega \rightarrow 0) = r_{td}^{(ss)} + r_p^{(ss)} = r_{rec}^{(ss)} \quad (51)$$

To identify the low frequency capacitance we take the admittance

$$Y = i\omega C_{\mu}^{(cb)} + \left[r_{rec}^{(cb)}\right]^{-1} + Z_{ss}^{-1} \quad (52)$$

and calculate the low frequency limit of Z_{ss}^{-1} . The result is

$$Y(\omega \rightarrow 0) = \frac{1}{r_{rec}^{(cb)}} + \frac{1}{r_{rec}^{(ss)}} + i\omega C_{\mu}^{(cb)} + i\omega B C_{\mu eq}^{(ss)} \quad (53)$$

The low frequency limit is a parallel (r_{rec} , C_{lf}) circuit. The total resistance is a parallel of the recombination resistances of the two charge transfer channels, as indicated in Eq. (20) and illustrated in Fig. 2c:

$$r_{rec}^{-1} = k_{cb} C_{\mu}^{(cb)} + k_{ss} C_{\mu}^{(ss)} \quad (54)$$

The low frequency capacitance is

$$C_{lf} = C'(\omega \rightarrow 0) = C_{\mu}^{(cb)} + B C_{\mu eq}^{(ss)} \quad (55)$$

and it is positive, so that the impedance spectrum approaches the real axis from above, and no inductive loop is present in this model. The effect of the inductor is to increase the value of capacitance and increase the resistance, as indicated in Eqs. (43) and (44). Therefore, the presence of charge transfer *reduces* the value of the low frequency trap capacitance from the equilibrium value $C_{\mu eq}^{(ss)}$, to

$$C_{\mu lf}^{(ss)} = \frac{\varepsilon_r + \bar{f}_{ss} k_{ss}}{\varepsilon_r + k_{ss}} C_{\mu eq}^{(ss)} \quad (56)$$

Note also that if $k_{ss} = 0$ both circuits in Fig. 2b and c for the trap with charge transfer reduce to the standard circuit for a trap, which is a series ($r_{td}^{(ss)}$, $C_{\mu eq}^{(ss)}$) [9,20]. Finally, we calculate the apparent electron lifetime which is given by Bisquert et al. [23]

$$\tau_n = r_{rec} C_{lf} = \frac{C_{\mu}^{(cb)} + B C_{\mu eq}^{(ss)}}{k_{cb} C_{\mu}^{(cb)} + k_{ss} C_{\mu eq}^{(ss)}} \quad (57)$$

2.6. Exponential distribution of surface states

Let us consider a distribution of surface states $g(E)$ and calculate the corresponding capacitance. If we assume that the trapping constant β_c is the same for all the states in the distribution, then the rate constant for electron release $\varepsilon_r(E)$ increases rapidly at increasing energies. If k_{ss} is constant or decreases upwards in energy, there is a point where $\beta_c \varepsilon_r(E_d) = k_{ss}$ that is called the demarcation energy, E_d [17].

Since the impedances of the different surface states are connected in parallel, we can add the frequency-dependent capacitance, $C_{ss}^*(\omega) = 1/i\omega Z_{ss}(\omega)$, corresponding to each interval of energy dE , as follows [20]:

$$C_{ss}^*(\omega) = \int_{E_v}^{E_c} C_{\mu eq}^{(ss)}(E) \frac{1 + k_{ss}/i\omega}{1 + i\omega/\omega_t} dE \quad (58)$$

where $C_{\mu eq}^{(ss)}(E)$ is the equilibrium chemical capacitance per unit energy in the interval of energy dE ,

$$C_{\mu eq}^{(ss)}(E_F, E) = \frac{q^2}{k_B T} g(E) \bar{f}_{ss} (1 - \bar{f}_{ss}) \quad (59)$$

The low frequency capacitance will be given by

$$C_{\mu lf}^{(ss)}(E_F) = \int_{E_v}^{E_c} \frac{\varepsilon_r(E) + \bar{f}_{ss} k_{ss}}{\varepsilon_r(E) + k_{ss}} C_{\mu eq}^{(ss)}(E) dE \quad (60)$$

and the dc resistance is

$$\left[r_{rec}^{(ss)}\right]^{-1} = \frac{q^2 L}{k_B T} \int_{E_v}^{E_c} k_{ss} g(E) \bar{f}_{ss} (1 - \bar{f}_{ss}) dE \quad (61)$$

We assume the specific case of an exponential distribution [8,23] defined as

$$g(E) = \frac{N_{ss}}{k_B T_0} \exp[-(E_c - E)/k_B T_0] \quad (62)$$

Here, T_0 is a parameter with temperature unit that defines the depth of the distribution below E_c .

3. Discussion

We first analyze the occupancy of the surface state as a function of the free electron Fermi level, E_F , see Fig. 3. If the rate of charge transfer is low, with respect to detrapping time ($k_{ss} \ll \varepsilon_r$), the surface state follows the usual statistics so that the occupancy increases at $E_F = E_t$. However, if $k_{ss} \gg \varepsilon_r$, the trap is filled only when E_F is substantially higher than E_t [16].

The trap characteristic frequency has been given in Eq. (31) and is shown in Fig. 3 as a function of E_F . The trap frequency is composed of the reciprocal of three time constants for trapping, detrapping, and charge transfer, and the shorter time constant dominates ω_t . When the occupancy is $f_{ss} < 1/2$, ω_t is governed by the larger of either ε_r or k_{ss} . When $f_{ss} > 1/2$, the fastest process is detrapping, so that $\omega_t = \beta_c n_c$ and it increases rapidly with increasing E_F .

Interpretation of experimental IS results requires the determination of equivalent circuit parameters as a function of bias voltage. Fig. 4 shows the predicted evolution of such parameters. First, Fig. 4a shows the shape of the chemical capacitance. For the low charge transfer rate ($k_{ss} \ll \varepsilon_r$), the low frequency capacitance simply follows the shape of the equilibrium chemical capacitance. Such shape, as is well known, consists on a peak at the point of the half occupation of the surface state and a further exponential increase due to the conduction band capacitance. However, at high charge transfer rate ($k_{ss} \gg \varepsilon_r$), we find a different result. Here the capacitance measured at low frequency is, at low occupation ($f_{ss} < 1/2$), considerably less than the equilibrium capacitance of the trap. This result was expressed in Eq. (56) and is well illustrated in Fig. 4a. The reason for this decrease is that the response of the trap is controlled by charge transfer, as mentioned above, and therefore a displacement of the Fermi level produces a loss of carriers, in comparison to the case in which the number of carriers is conserved. Therefore, this result is not exclusively related to the IS measurement, but quite generally, the measurement of the quasi-equilibrium capacitance by any method will provide a departure from the equilibrium capacitance of Eq. (24).

The recombination (charge transfer) resistance in Fig. 4b also shows interesting features. The general tendency of $r_{rec}^{(ss)}$ is an expo-

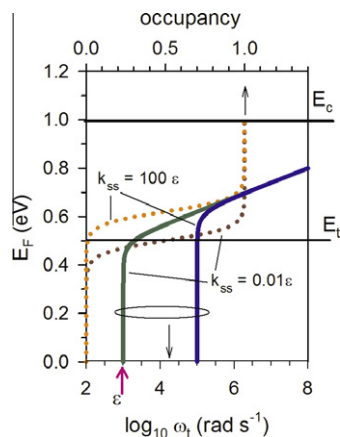


Fig. 3. (a) Representation of the occupancy of the trap state (top axis) at $E_t = 0.5$ eV and the characteristic trap frequency (bottom axis) as a function of the Fermi level of free electrons (left axis) at $T = 300$ K. Two cases are shown according to the factor between the rate of charge transfer k_{ss} and the time constant for detrapping, $\varepsilon_r = 10^3$ s $^{-1}$.

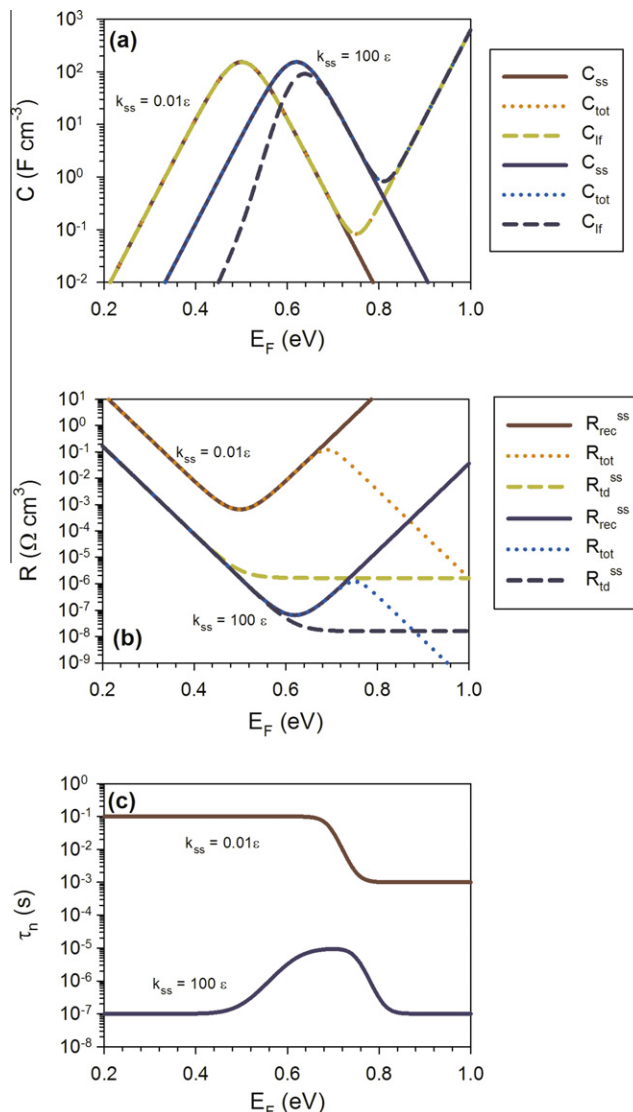


Fig. 4. Representation of (a) capacitances (b) resistances and (c) apparent electron lifetime, as a function of the free electron Fermi level, for a surface state at $E_t = 0.5$ eV ($N_{ss} = 10^{20}$ cm $^{-3}$) and conduction band at $E_c = 1$ eV ($N_c = 10^{20}$ cm $^{-3}$) at $T = 300$ K. Two cases are shown according to the factor between the rate of charge transfer k_{ss} and the time constant for detrapping, $\varepsilon = 10^3$ s $^{-1}$. The rate of transfer from the conduction band is $k_{cb} = 100k_{ss}$.

ponential decrease and later increase, with the minimum at the point where the surface state is half occupied [16]. In accordance with Fig. 3 the minimum shifts to higher voltage when the charge transfer rate constant increases. If $k_{ss} \gg \varepsilon_r$, in the decreasing part, i.e. at $f_{ss} < 1/2$, the recombination resistance is controlled by the trapping resistance, $r_{rec}^{(ss)} \approx r_{td}^{(ss)}$, see Eq. (42).

The changes in low frequency capacitance and recombination resistance produce also variations in the apparent electron lifetime, defined in Eq. (57), see Fig. 4c. If the rate of charge transfer is low, the lifetime makes a simple transition from the value of surface states to the value of conduction band electrons. But if $k_{ss} \gg \varepsilon_r$, there is an additional increase at low voltage due to the fact that the low frequency capacitance is lower than equilibrium capacitance. These results are based on an apparent lifetime $\tau_n = r_{rec} C_{lf}$ which must be regarded as an operational definition. Indeed we will see below that the frequency response of the model is not a simple RC arc, which means that the small perturbation decay [23] is not an exponential; it contains additional features, and

the issue of the lifetime must be carefully defined if required. The physical reason for this is the following. In the simplest model of a solar cell (which is described by RC arc [23]), the measurement of the electron lifetime means the discharge of the chemical capacitance via the recombination resistance, and this clearly provides the exponential decay of excess carrier density. If the solar cell is composed of a distribution of bandgap states, but their equilibration with the conduction band is fast, we have also an RC arc implying exponential decay, although the capacitance is increased, and also the lifetime, by the capacitance of the bandgap states; this is the basis for the quasistatic approximation [23,34]. However in the situation of Fig. 2b, the traps dynamics is not trivialized, and additional effects may happen. If the resistance for trapping–detrapping is not small, part of the dynamics is the flow of the charges from the conduction band capacitance to the trap capacitance, and another part is the discharge via the recombination resistances.

We turn our attention to the parameters that are measured for an exponential distribution of states. For simplicity we assume that k_{ss} is the same for all the states in the distribution, so that we may focus on the features that depend on the occupation of the surface state. We recall that the equilibrium capacitance of the distribution, is given approximately by the density of states [30]

$$C_{\mu eq}^{(ss)}(E_F) = \int_{E_v}^{E_c} C_{\mu eq}^{(ss)}(E_F, E) dE \approx q^2 g(E_F) \quad (63)$$

In Fig. 5a, we readily notice that below the demarcation level, the low frequency capacitance is considerably less than the equilibrium value of Eq. (63), and Fig. 5b shows that the charge transfer resistance is higher than the value obtained when the occupation of the state is low. These variations produce a step in the apparent electron lifetime, as shown in Fig. 5c.

Another central tool for the experimental interpretation of IS is the analysis of the frequency spectra. We show in Fig. 6 the simulated spectra of the impedance model in the complex impedance plane, and the situation of the characteristic frequencies of the model in the spectra. First Fig. 6a shows the features of the surface state subcircuit, Z_{ss} . The model circuit of Fig. 2b indicates that the spectrum is an RC arc that is shifted along the real axis by the trapping–detrapping resistance. At the top of the arc is the frequency of the recombination rate constant k_{ss} . When we include the Z_{ss} in the framework of the general equivalent circuit, we obtain different types of spectra according to the slowest characteristic frequency. If k_{ss} is small we observe the relaxation of the trap at low frequency, and the arc of the conduction band at the high frequency part of the spectra, Fig. 7b. However if k_{ss} is large, there is a single skewed arc, due to the relaxation of conduction band electrons, modified by the surface state at high frequencies.

As mentioned in the previous section, the model of recombination via bandgap states, consistent with detailed balance, cannot produce a negative capacitance at any frequency, despite the appearance of inductors in the equivalent circuit. This is consistent with very general equivalent circuits for recombination in semiconductors developed long ago [35]. Recently, the observation of the negative capacitance in organic photovoltaic devices was attributed to recombination [36]. However, in my view a proper model of the negative capacitance based on the known properties of recombination of carriers in semiconductors is not available. The above calculations in this paper show that recombination alone does not produce this behaviour, and another process is required that produces the loop of the impedance at low frequency. Models for the charge injection at the metal–organic interface do produce the negative capacitance, but such effect requires a mechanism of displacement of the energetics of the surface state [37,38].

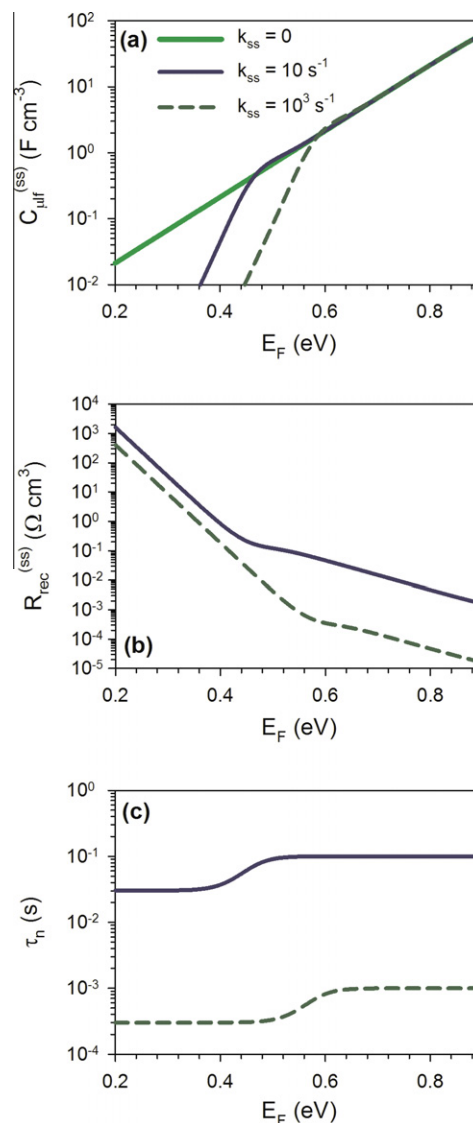


Fig. 5. Representation of (a) low frequency capacitance (b) recombination resistance and (c) apparent electron lifetime, as a function of the free electron Fermi level, for an exponential distribution of surface state states. Three cases are shown according to the value of the rate of charge transfer k_{ss} , which is independent of energy. Parameters used in the calculation: $T = 300$ K, $E_c = 1$ eV, $T_0 = 1000$ K ($\alpha = T/T_0 = 0.33$), $N_c = 10^{18}$ cm $^{-3}$, $N_{ss} = 10^{20}$ cm $^{-3}$, $\beta = 10^{-10}$ cm 2 s $^{-1}$.

Even though the full thermodynamic-kinetic model for the recombination via surface states does not provide a negative capacitance, we can still explore $B < 0$ in Eq. (43) as a formal possibility that may be eventually validated in some different kind of model. The resulting impedance spectra are shown in Fig. 7. The trap impedance occurs in the fourth quadrant, Fig. 7a, and the full impedance model including conduction band components, may consist on either a normal positive response in the first quadrant, Fig. 7c, or an arc that loops in the fourth quadrant at the lowest measurement frequencies, Fig. 7b. This last shape is quite characteristic of the IS measurements in some types of DSC [24,27].

As final remarks we should indicate additional important effects that occur in the application of the model in DSC devices, but have been neglected in the former discussions to simplify the treatment. The first is the influence of a constant capacitance at the surface of the nanostructured semiconductor, which is combined in series to the chemical capacitances discussed above. This may originate in the Helmholtz capacitance that is always

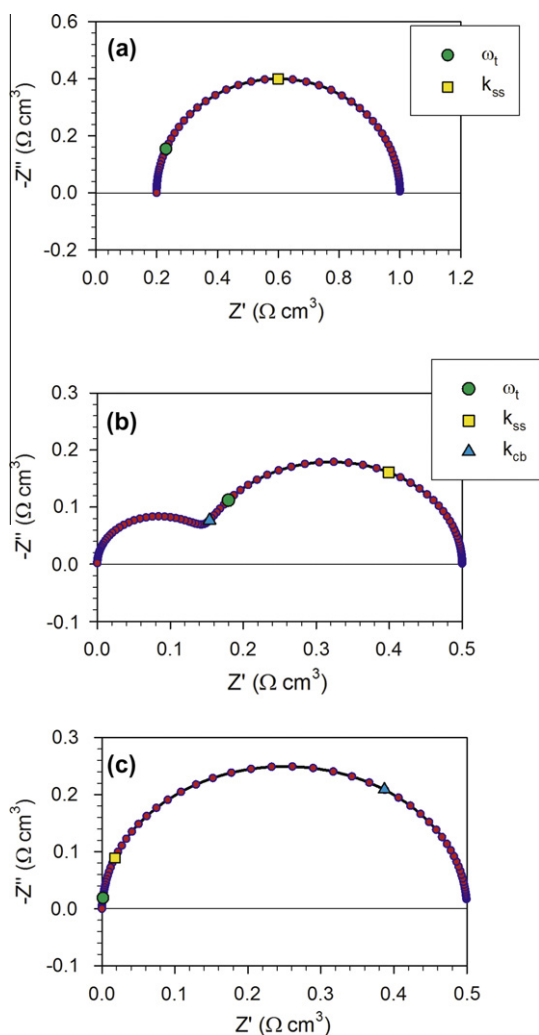


Fig. 6. Representation of the impedance in the complex plot, indicating selected frequencies. (a) The traps subcircuit, Z_{ss} , Fig. 2b for parameters $r_{rec}^{(ss)} = 1 \Omega$, $C_{\mu}^{(ss)} = 1 \text{ F}$, $B = 0.8$, ($k_{ss} = 1 \text{ s}^{-1}$, $\omega_t = 5 \text{ rad s}^{-1}$). (b and c) The total impedance, including capacitance and charge transfer resistance of the conduction band, Fig. 2a. Parameters: (b) $r_{rec}^{(cb)} = 1 \Omega$, $C_{\mu}^{(cb)} = 0.1 \text{ F}$ ($k_{cb} = 10 \text{ s}^{-1}$). (c) $r_{rec}^{(cb)} = 1 \Omega$, $C_{\mu}^{(cb)} = 10 \text{ F}$ ($k_{cb} = 0.1 \text{ s}^{-1}$).

present at the semiconductor/electrolyte interface, with possible contribution from the organic layer constituted by the photoactive dye and other coabsorbants, or additionally, by inorganic covering thin layers that are used to improve the performance of the device. A charging of the surface state in the presence of the dielectric capacitance fixes the Fermi level in the bandgap, and a variety of behaviours are possible, depending on the values of the chemical capacitance for the bulk semiconductor, of the surface states, and of the dielectric capacitance. One important situation is that in which the capacitance remains constant until the surface states are completely filled. These effects were recently discussed in detail in connection with quantum dot-sensitized solar cells [24].

Since the effects of surface states appear in the low frequency side of the IS measurements, it is very likely that they become mixed with the diffusion in the electrolyte (especially if it is highly viscous) or hole conductor, since the hole transport rate in these media tends to be low [27]. This problem may become complex, as the interfacial charge transfer is coupled with the diffusion of both electrons and holes. Especially important in order to evaluate modelling results is to determine the distribution of the applied

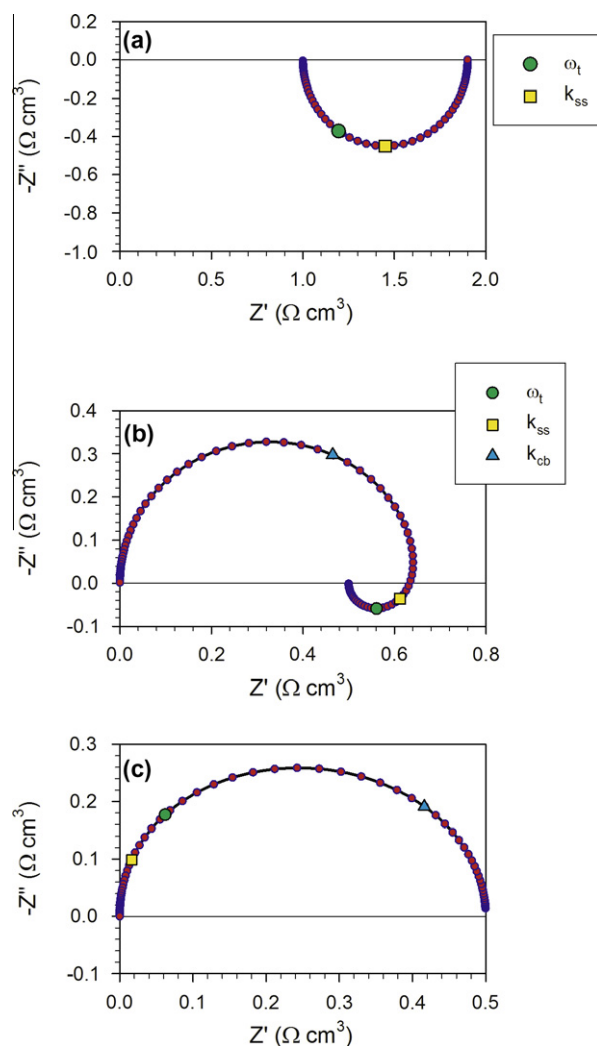


Fig. 7. Representation of the impedance in the complex plot, indicating selected frequencies. (a) The traps subcircuit, Z_{ss} , Fig. 2b for parameters $r_{rec}^{(ss)} = 1 \Omega$, $C_{\mu}^{(ss)} = 1 \text{ F}$, $B = -0.9$, ($k_{ss} = 1 \text{ s}^{-1}$, $\omega_t = 0.52 \text{ rad s}^{-1}$). (b and c) The total impedance, including capacitance and charge transfer resistance of the conduction band, Fig. 2a. Parameters: (b) $r_{rec}^{(cb)} = 1 \Omega$, $C_{\mu}^{(cb)} = 0.1 \text{ F}$ ($k_{cb} = 10 \text{ s}^{-1}$). (c) $r_{rec}^{(cb)} = 1 \Omega$, $C_{\mu}^{(cb)} = 10 \text{ F}$ ($k_{cb} = 0.1 \text{ s}^{-1}$).

potential in different contributions either for driving transport or increasing the Fermi level.

4. Conclusions

We have outlined a model for the electronic behaviour of a nanostructured semiconductor permeated with a highly conducting hole transport material, to evaluate the kinetic (frequency) behaviour and quasistatic quantities due to charge transfer via surface states. Solving the model for steady state as well as ac conditions, shows that dc resistances, can be simply guessed from steady state recombination current. The ac response of this system allows for different pictures in terms of equivalent circuits, but all of them introduce a parallel resistance to the standard RC series circuit of a trap that only communicates with the conduction band (in the absence of charge transfer). At each value of the steady state Fermi level, the characteristic frequency of the trap is determined by the fastest time constant, either trapping, detrapping or interfacial charge transfer. Another major conclusion is that if the rate of charge transfer is large, the low frequency (measurable) capacitance of the trap is less than the thermodynamic equilibrium

capacitance. Finally, it is shown that the complete circuit for the recombination via surface state, based on detailed balance kinetics and standard semiconductor statistics, cannot provide negative capacitance components. Nonetheless, a formal extension of the model shows impedance spectra that are quite similar to those measured in several kinds of dye-sensitized solar cells.

Acknowledgments

It is a pleasure to dedicate this paper to Prof. Laurie Peter, master and friend, in recognition to his pioneering and continuing contributions in these topics, and to the high quality of his work, which has guided many of us.

We thank financial support from Ministerio de Ciencia e Innovación under Project HOPE CSD2007-00007 and Generalitat Valenciana under Project PROMETEO/2009/058.

References

- [1] L.M. Peter, *J. Phys. Chem. C* 111 (2007) 6601.
- [2] J. Li, L.M. Peter, *J. Electroanal. Chem.* 165 (1984) 29.
- [3] J. Li, R. Peat, L.M. Peter, *J. Electroanal. Chem.* 165 (1984) 41.
- [4] J. Li, L.M. Peter, *J. Electroanal. Chem.* 193 (1985) 27.
- [5] C. Gutierrez, P. Salvador, *J. Electrochem. Soc.* 133 (1986) 924.
- [6] J. Bisquert, *Phys. Chem. Chem. Phys.* 10 (2008) 3175.
- [7] A.C. Fisher, L.M. Peter, E.A. Ponomarev, A.B. Walker, K.G.U. Wijayantha, *J. Phys. Chem. B* 104 (2000) 949.
- [8] Q. Wang, S. Ito, M. Grätzel, F. Fabregat-Santiago, I. Mora-Seró, J. Bisquert, T. Bessho, H. Imai, *J. Phys. Chem. B* 110 (2006) 19406.
- [9] E.H. Nicollian, A. Goetzberger, *Bell Syst. Technol. J.* 46 (1967) 1055.
- [10] F. Cardon, *Physica* 57 (1972) 390.
- [11] P. Allongue, H. Cachet, *J. Electroanal. Chem.* 176 (1984) 369.
- [12] Z. Hens, *J. Phys. Chem. B* 103 (1999) 122.
- [13] Z. Hens, W.P. Gomes, *J. Phys. Chem. B* 103 (1999) 130.
- [14] K. Kobayashi, M. Takata, S. Okamoto, *J. Electroanal. Chem.* 185 (1984) 47.
- [15] D. Vanmaekelbergh, *Electrochim. Acta* 42 (1997) 1135.
- [16] I. Mora-Seró, J. Bisquert, *Nano Lett.* 3 (2003) 945.
- [17] J. Bisquert, A. Zaban, P. Salvador, *J. Phys. Chem. B* 106 (2002) 8774.
- [18] P. Salvador, M. González-Hidalgo, A. Zaban, J. Bisquert, *J. Phys. Chem. B* 109 (2005) 15915.
- [19] J. Bisquert, V.S. Vikhrenko, *Electrochim. Acta* 47 (2002) 3977.
- [20] J. Bisquert, *Phys. Rev. B* 77 (2008) 235203.
- [21] R. Kern, R. Sastrawan, J. Ferber, R. Stangl, J. Luther, *Electrochim. Acta* 47 (2002) 4213.
- [22] M. Adachi, M. Sakamoto, J. Jiu, Y. Ogata, S. Isoda, *J. Phys. Chem. B* 110 (2006) 13872.
- [23] J. Bisquert, F. Fabregat-Santiago, I. Mora-Seró, G. Garcia-Belmonte, S. Giménez, *J. Phys. Chem. C* 113 (2009) 17278.
- [24] I. Mora-Seró, S. Giménez, F. Fabregat-Santiago, R. Gomez, Q. Shen, T. Toyoda, J. Bisquert, *Acc. Chem. Res.* 42 (2009) 1848.
- [25] H. Randriamahazaka, F. Fabregat-Santiago, A. Zaban, J. García-Cañadas, G. Garcia-Belmonte, J. Bisquert, *Phys. Chem. Chem. Phys.* 8 (2006) 1827.
- [26] I. Mora-Seró, J. Bisquert, F. Fabregat-Santiago, G. Garcia-Belmonte, G. Zoppi, K. Durose, Y.Y. Proskuryakov, I. Oja, A. Belaidi, T. Dittrich, R. Tena-Zaera, A. Katty, C. Lévy-Clement, V. Barrioz, S.J.C. Irvine, *Nano Lett.* 6 (2006) 640.
- [27] T.C. Li, M.S. Góes, F. Fabregat-Santiago, J. Bisquert, P.R. Bueno, C. Prasittichaia, J.T. Hupp, T.J. Marks, *J. Phys. Chem. C* 113 (2009) 18385.
- [28] J. Bisquert, *Phys. Chem. Chem. Phys.* 5 (2003) 5360.
- [29] J. Bisquert, *J. Phys. Chem. B* 106 (2002) 325.
- [30] F. Fabregat-Santiago, I. Mora-Seró, G. Garcia-Belmonte, J. Bisquert, *J. Phys. Chem. B* 107 (2003) 758.
- [31] W. Shockley, W.T. Read, *Phys. Rev.* 87 (1952) 835.
- [32] J. Bisquert, D. Cahen, S. Rühle, G. Hodes, A. Zaban, *J. Phys. Chem. B* 108 (2004) 8106.
- [33] C. Nicolis, A. Babloyante, *J. Chem. Phys.* 51 (1969) 2632.
- [34] J. Bisquert, V.S. Vikhrenko, *J. Phys. Chem. B* 108 (2004) 2313.
- [35] P.C.H. Chan, C.T. Sah, M.F. Li, *IEEE Trans. Electron Dev.* 26 (1979) 924.
- [36] C. Lungenschmied, E. Ehrenfreund, N.S. Sariciftci, *Org. Electron.* 10 (2009) 115.
- [37] J. Bisquert, G. Garcia-Belmonte, A. Pitarch, H. Bolink, *Chem. Phys. Lett.* 422 (2006) 184.
- [38] G. Garcia-Belmonte, H. Bolink, J. Bisquert, *Phys. Rev. B* 75 (2007) 085316.